

Available online at [www.sciencedirect.com](http://www.sciencedirect.com)

ScienceDirect

journal homepage: [www.intl.elsevierhealth.com/journals/dema](http://www.intl.elsevierhealth.com/journals/dema)

# Bone healing with niobium-containing bioactive glass composition in rat femur model: A micro-CT study

Gabriela de Souza Balbinot<sup>a</sup>, Vicente Castelo Branco Leitune<sup>a</sup>,  
Deise Ponzoni<sup>b</sup>, Fabricio Mezzomo Collares<sup>a,\*</sup>

<sup>a</sup> Dental Materials Laboratory, School of Dentistry, Universidade Federal do Rio Grande do Sul, Porto Alegre, Brazil

<sup>b</sup> Oral and Maxillofacial Surgery Unit, School of Dentistry, Universidade Federal do Rio Grande do Sul, Brazil

## ARTICLE INFO

### Keywords:

Bone substitutes  
Animal models  
Bioactive glasses  
Niobium

## ABSTRACT

**Objective.** The aim of this study is to investigate bone healing ability of niobium-containing bioactive glasses in rat femur model with quantitative and qualitative measurements through x-ray computed microtomography.

**Methods.** Niobium-containing bioactive powders and scaffolds were produced by sol-gel route (BAGNb). Glasses without niobium addition were produced as well (BAG). Five groups were used: BAGNb powders, BAG powders, BAGNb scaffolds, BAG scaffolds and, as a control group, autogenous bone was used. Materials were implanted in the femur of male rats (Wistar Lineage n=10) and the healing was observed after 15, 30 and 60 days. After the post-operative times, samples were scanned by X-ray microcomputed tomography where morphometric measurements and the mineral density were assessed in image software.

**Results.** No postoperative complications were observed after surgery. BAGNb glasses presented higher mineral deposition, which was observed in the relative volume of bone and the mineral density when compared BAG groups. In these parameters, no statistical difference was found between BAGNb and autogenous bone. The BAGNb powders presented a higher amount of mineralized tissue when compared to BAGNb scaffolds. The analysis of trabecular structure showed lower trabecular formation in synthetic materials when compared to autogenous bone.

**Significance.** Niobium-containing bioactive glasses promoted bone formation comparable to that of the autogenous bone without compromising the quality of the formed bone.

© 2019 The Academy of Dental Materials. Published by Elsevier Inc. All rights reserved.

## 1. Introduction

Bioactive glasses are a class of synthetic materials that may be used in bone regeneration applications in dentistry [1,2]. The osteoinductive and osteoconductive abilities [3] of these glasses are related to their ion release that promotes bone

formation by way of two mechanisms, specifically 1) the formation of a carbonated hydroxyapatite layer in the surfaces of the particles [4] and 2) the upregulation of cell activity to stimulate the deposition of bone tissue [5]. Improvements in glass composition and structure may contribute to an improved release of bioactive ions and increased bone formation.

\* Corresponding author at: Rua Ramiro Barcelos, 2492 Porto Alegre, Rio Grande do Sul, Brazil.

E-mail address: [fabricio.collares@ufrgs.br](mailto:fabricio.collares@ufrgs.br) (F.M. Collares).

<https://doi.org/10.1016/j.dental.2019.07.012>

0109-5641/© 2019 The Academy of Dental Materials. Published by Elsevier Inc. All rights reserved.

The enhancement of bioactive glass composition and production may improve bone regeneration capacity. Niobium has been investigated as biomaterial to be used [6–9] due to its ability to promote mineral deposition [6,7,10,11]. The development of sol–gel-derived, niobium-containing bioactive glasses powders and scaffolds was previously shown [7] and increased mineralization ability was observed for niobium-containing grafts in vitro.

Several approaches are used to promote the reestablishment of bone tissue for prosthetic rehabilitation, while autogenous bone remains the gold standard graft for maxillae and mandible reconstructions [12–15]. Synthetic bone substitutes have been used as alternatives that have ensured reduced patient morbidity [13] and comparable bone formation [14]. The placement of dental implants in edentulous patients is additionally related to improved health parameters and an increased quality of life, but may be limited in terms of efficacy by the absence of adequate quality and quantity of bone [15]. The aim of this study was to investigate the bone healing ability of niobium-containing bioactive glasses in a rat femur model according to quantitative and qualitative measurements obtained through X-ray computed microtomography. The working hypothesis is that the addition of niobium increased the bone regeneration ability promoted by sol-gel derived bioactive glasses.

## 2. Materials and methods

### 2.1. Bioactive glass preparation

Bioactive glass powders and scaffolds were prepared as described previously [7]. Briefly, the sol–gel route was used, incorporating tetraethylorthosilicate (TEOS), triethyl phosphate (TEP), calcium nitrate ( $\text{CaNO}_3$ ), sodium nitrate ( $\text{NaNO}_3$ ), and niobium chloride ( $\text{NbCl}_5$ ) for the preparation of niobium-containing bioactive glasses (BAGNb). Glasses without niobium (BAG) were produced as well. Glass powders were obtained after heat treatment at 70 °C, 120 °C, and 700 °C for 24 h per each temperature point. The particle size used ranged between 300  $\mu\text{m}$  and 600  $\mu\text{m}$ . For scaffold synthesis, the sol was produced as described for powders, while porous gels were obtained via a foaming process with a surfactant (sodium lauryl sulfate; Biodinamica, Parana, Brazil) and a catalyst (fluoridric gel 5%; Neon, São Paulo, Brazil). After heat treatment, scaffold cylinders measuring 2 mm in diameter by 2 mm in height were obtained. All materials were sterilized in an autoclave prior to the surgery.

### 2.2. Study design

This study was developed in accordance with the ARRIVE guidelines. Male rats (*Rattus Novegicus Albinus*, *Rodentia Mammalia*—Wistar lineage) with an average weight of 500 g were used. All animals ( $n=10$ ) were maintained in appropriate cages in a controlled temperature range (20 °C–24 °C) and light/dark cycle with food and water provided ad libitum. All procedures were performed according to the Guide for the Care and Use of Laboratory Animals and with approval from the ethical committee of Porto Alegre University Hos-

pital (Porto Alegre, Brazil). All procedures were performed at the Center of Animal Experimentation of Animals Porto Alegre University Hospital (Porto Alegre, Brazil). Animals were divided, by a blinded veterinary, according to body weight into five groups, as follows: a control group (autogenous bone removed from the femur when the defect was made and replaced in the cavity); a BAGNb powder group (glass powders with niobium addition); a BAG powder group (glass powders without niobium addition); a BAGNb scaffold group (glass scaffolds with niobium addition); and a BAG scaffold group (glass scaffolds with niobium addition).

### 2.3. Surgical procedure

The surgical procedure was performed after anesthesia with an intraperitoneal administration of ketamine (50 mg/kg), xylazine (5 mg/kg), and 1%–2% vaporized isofluorane for maintenance. After anesthesia, shaving and antiseptics were carried out on the leg to be operated on and local anesthesia was established close to the surgical site with bupivacaine 5%/adrenaline 1:200,000. A 3-cm-long incision was made on the anterolateral surface of the leg. The muscles were dissected and the proximal diaphysis of the femur was reached. One defect measuring 2 mm in diameter by 2 mm in height was produced in each rat using a trephine bur. The materials were inserted in the produced defect according to the aforementioned groups. In the control group, the autogenous bone removed upon drilling was inserted back into the defect. The fascia–periosteal flaps were sutured with 4.0 glycolide/L-lactide copolymer (Vicryl®; Ethicon, Somerville, NJ, USA) and the skin was sutured with 4.0 nylon. Postoperative analgesia was performed immediately after the surgery with a single dose of morphine (5 mg/kg) administered via intraperitoneal injection and tramadol (20 mg/kg) during five days in a 12/12-h on/off cycle. The removed samples were stored in 10% formalin.

### 2.4. X-ray computed microtomography

Samples were evaluated via X-ray computed microtomography (MicroCT.SMX-90 CT; Shimadzu Corp., Kyoto, Japan). The standardization of the samples was performed by sectioning the femurs in their long axes at points 2 mm away from the defect in the epiphysis and diaphysis directions. Samples were gently washed with distilled water for 30 s and mounted in a rotary stage, where images were taken in a 360° rotation with a 60 kV intensity. The images were then reconstructed in the inspeXio SMX-90CT software program (Shimadzu Corp., Kyoto, Japan) with a 10  $\mu\text{m}$  voxel size in images with a 512 × 512-pixel resolution and a 10  $\mu\text{m}$  thickness, which resulted in 268 images per sample. Measurements were performed in an image software program (ImageJ; National Institutes of Health, Bethesda, MD, USA), where images were used for the assessment of new bone formation. The measurements were performed by two trained examiners that were submitted to with submission to an interclass correlation coefficient (ICC) test prior to the analysis. A standard area in the cortical portion of the bone was selected and a color threshold was applied to the segmentation of different grey values in the images (Fig. 1). To select the threshold, an extra femur sample was

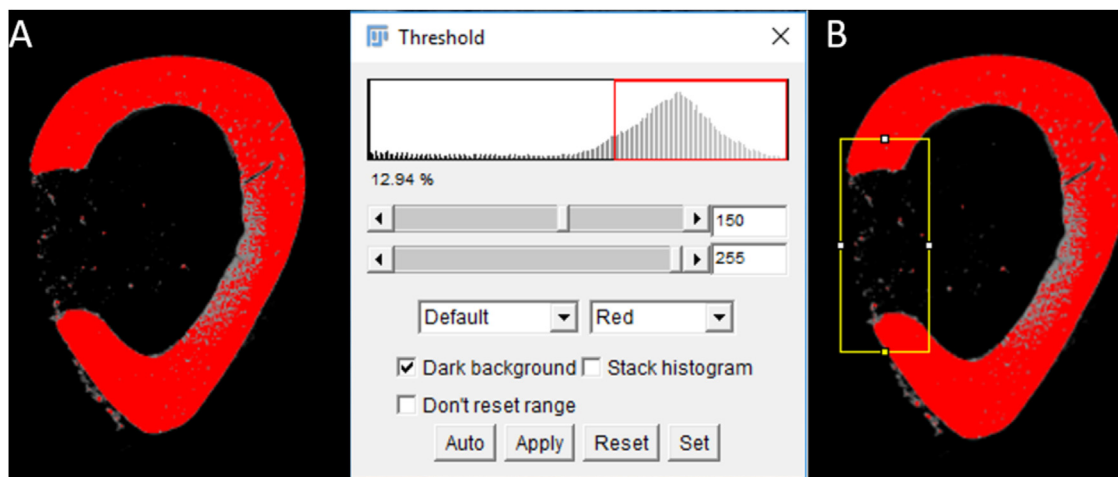


**Fig. 1** – Representative images of the parameters used in the analysis. **Fig. 1A** represents the model used to determine the threshold value between grey intensities to exclude the materials from the analysis. **Fig. 1B** shows the standardized area of the cortical portion of bone where measurements were performed.

filled with material and scanned with the same parameters used for the samples. This sample was used as a model to calculate the grey intensity of materials in the analysis (Fig. 1A). Based on these, the threshold was set in at 150 to 255 as shown in Fig. 1. A standardized area was used to select a region of interest (ROI) in the cortical portion of the bone (Fig. 1B). Bone density, trabecular thickness (Tb.Th), trabecular separation (Tb.Sp), and bone fraction (BV/BT) were measured with BoneJ plugin [16]. The area of bone, the volume of bone, and the percentage of bone in the defects were measured in the stack of images obtained in the analysis.

## 2.5. Statistical analysis

An ICC test was performed to assess the reliability of the analyses. The ICC analysis was performed in either an intrarater or interrater manner depending on the test. Random effects were used to calculate the ICC. The sample size was calculated based on previous studies [17,18] considering the minimum detectable difference in means of the observed effect size. The mineral density along the bone defect was descriptively analysed. Normality of the data was assessed using the Komolgorov–Smirnov test. Comparisons among different groups and postoperative times in terms of the area, the percentage of area, the volume, and mineral density were performed with two-way analysis of variance and the Tukey post-hoc test. For morphometric data, the nonparametric Kruskal–Wallis and Dunn tests were used to perform the analysis between groups and postoperative times. All tests were performed at a 5% significance.

## 3. Results

The intraoperative and postoperative periods during the study were followed by a veterinarian and no complications related to the procedure were observed. No bone fracture was noted during the postoperative period. The involved animals recovered well from the surgery without any loss of mobility. One

animal was excluded due to low body weight; furthermore, one animal was lost during the study due to wound complications, two animals were lost due to fracture of the femur during an autopsy after 15 days of surgery, and one animal presented malformation of the femoral condyle detected during the autopsy. These samples were excluded from the final evaluation. One hundred seventy-five samples were then analyzed in the present study. The ICC values were considered in intraexaminer and interexaminer manners. Interrater analysis showed good correlation (0.6–0.74.  $p < 0.05$ ) between examiners. The intrarater analysis showed good (0.6–0.74.  $p < 0.05$ ) and excellent (0.75–1.00.  $p < 0.05$ ) correlation.

The morphometric measurements were shown in Figs. 2 and 3. The relative volume of calcified tissue in the selected volume of interest (BV/TV) is shown in Fig. 2A. the longer the postoperative time, the higher the percentage of volume occupied by bone. After 15 days, only the BAGNb powder presented values similar to the autogenous bone. After 30 days, BAGNb powders and scaffolds reached the BV/TV of bone volume of the autogenous group. After 60 days, the autogenous bone group presented median values of 87.43% (87.05%–87.90%) of the volume covered by newly formed bone, which was significantly higher than the values found in other groups. The ConnD values for BAGNb and BAG powders were similar to those of the autogenous group after 15 days. After 30 days, no statistical difference was found between the materials and autogenous bone. After 60 days, BAG scaffolds presented reduced connectivity values when compared to at 30 days and to the other groups.

The analysis of trabecular structure is presented via the Tb.Sp, Tb.Th and Tb.N measurements in Fig. 3. No statistical difference was found between groups and postoperative times regarding the Tb.Sp values ( $p > 0.05$ ). For Tb.Th at 15 days, BAGNb powders and BAGNb scaffolds presented increased Tb.Th in comparison with the BAG groups (Fig. 3B;  $p < 0.05$ ), with no statistically significant difference between BAGNb materials and the autogenous bone. After 30 days after surgery, the obtained values were similar to the ones found

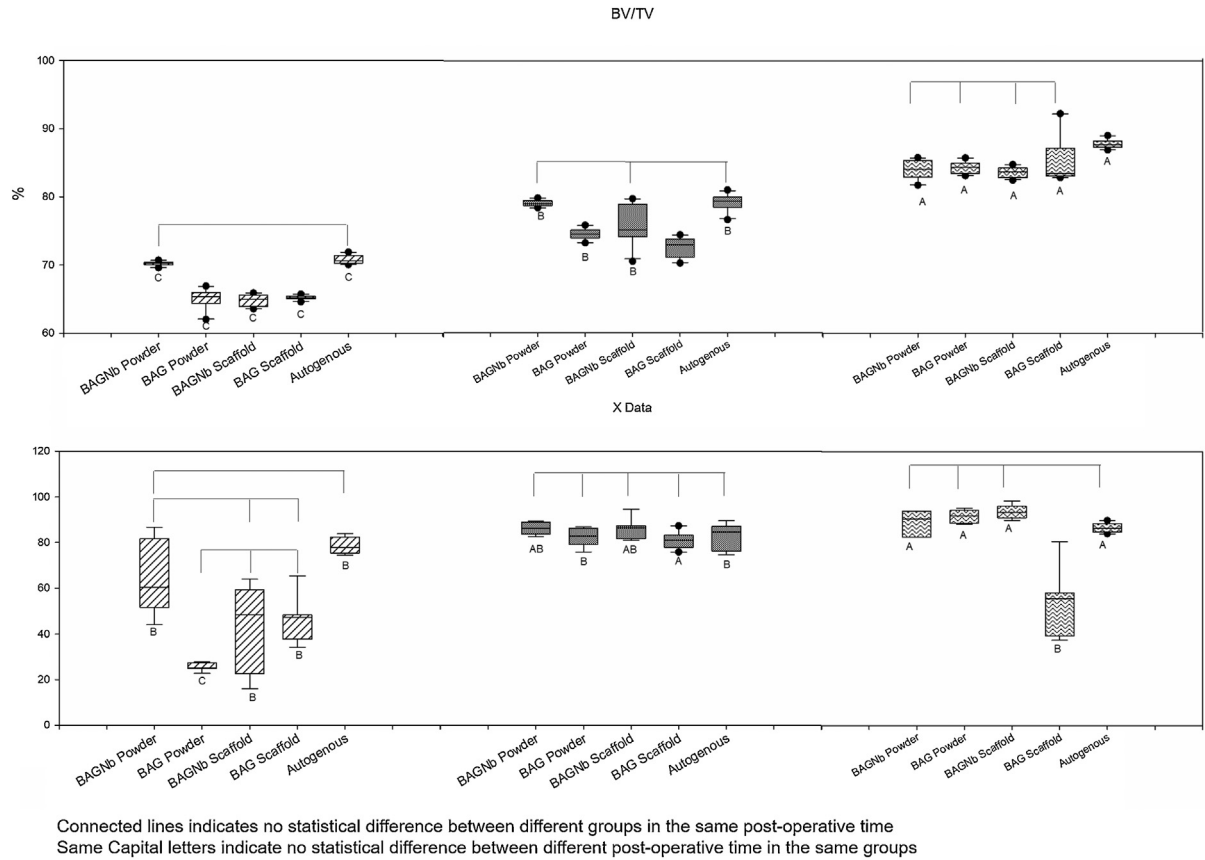


**Fig. 2 – The relative volume of calcified tissue in the selected volume of interest (BV/TV) and the degree to which parts of the object are multiply connected (ConnD) of the formed bone after 15, 30 and 60 days of surgery.**

at 60 days for all tested groups. The average number of trabeculae per unit length (Tb.N) at 15 days was similar for all groups (Fig. 3C;  $p > 0.05$ ). After both 30 and 60 days, autogenous bone presented a higher number of trabecula ( $p < 0.05$ ).

Mineral density is presented in Fig. 4 and Table 1. It is observed that mineral density in the center of the defect presented lower bone density values in all post-operative times. The difference between the bone density in the surrounding area and the density along the defect was higher after 15 days of surgery and the mean values were statistically lower for all groups (Table 1;  $p > 0.05$ ). Autogenous bone presented a higher density after 15 days of surgery. No statistical difference was found regarding density at 30 days versus 60 days for BAGNb powders and BAGNb scaffolds. Additionally, after 30 and 60 days, no statistical difference was observed between groups ( $p > 0.05$ ).

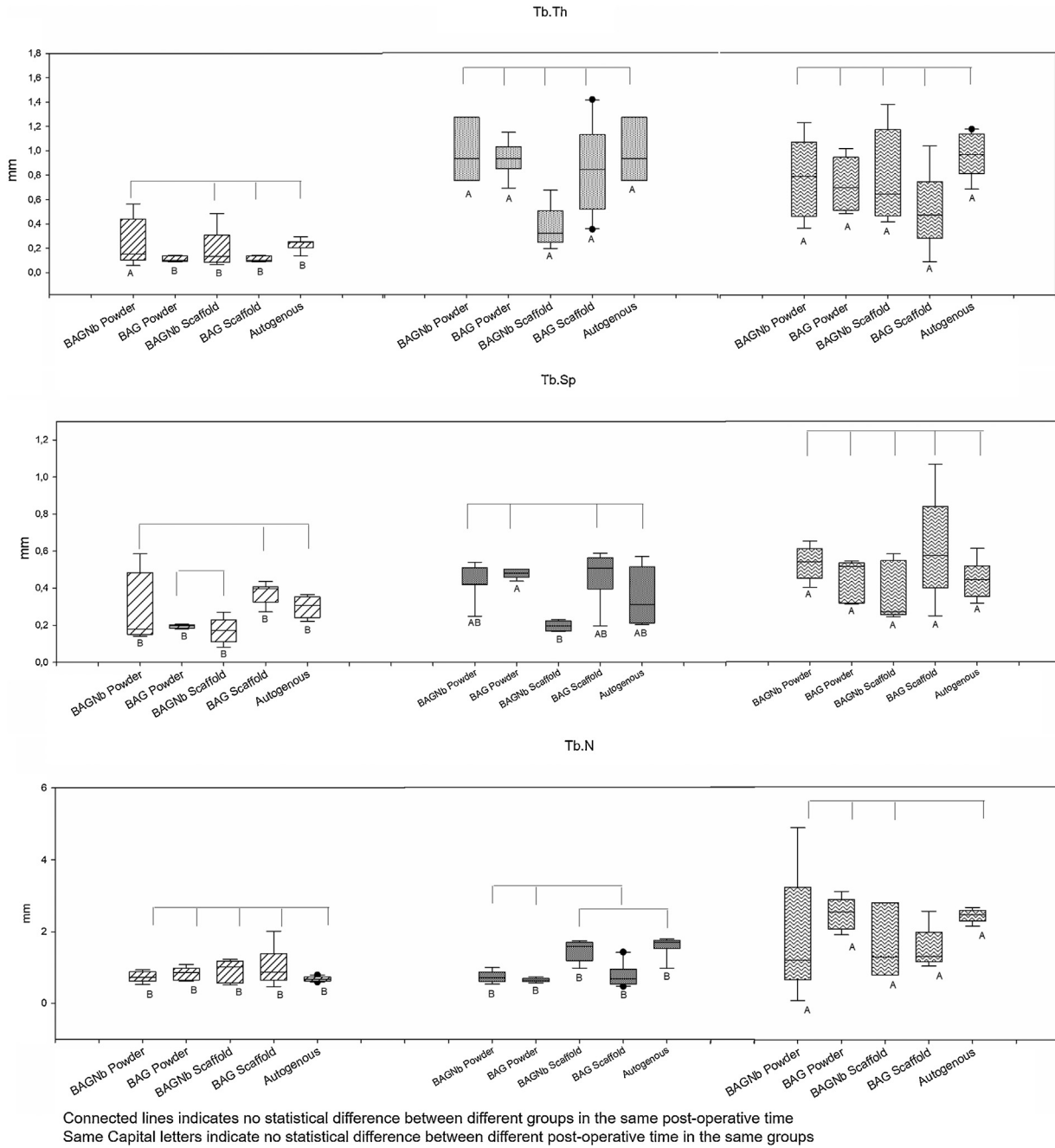
The area of bone, the volume of bone, and the percentage of bone in the defect are shown in Fig. 5. No statistical difference was found among the different groups in each post-operative time when the area (Fig. 5A), the percentage of the area (Fig. 5B), and volume (Fig. 5C) were considered. The values were high for 60 days as compared with at 15 days in all experimental groups ( $p < 0.05$ ). After 60 days of follow-up, the mean area of bone for the BAGNb powder, BAGNb scaffold, and BAG scaffold groups showed no statistical difference in comparison with the values found at 30 days. This was observed

for the BAGNb powder and BAGNb scaffolds considering the results of the percentage of area and volume (Fig. 5B and C, respectively).

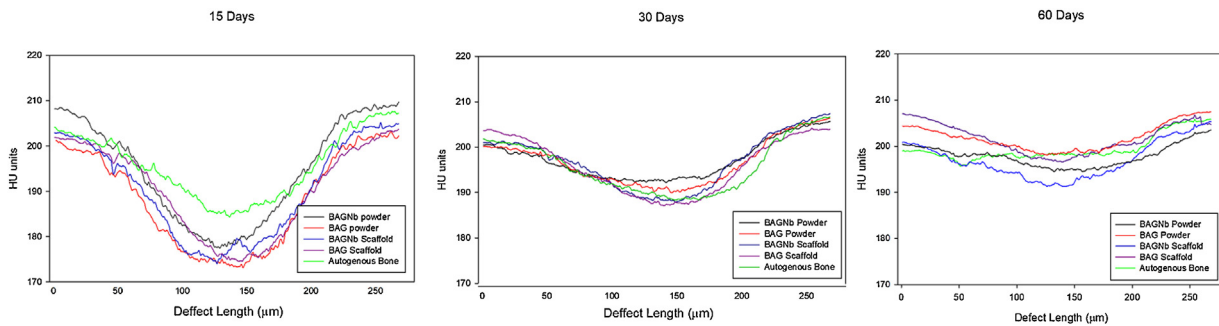
#### 4. Discussion

The quality and the quantity of bone is a determining factor for rehabilitation success when dental implants [19,20] are used. These are key parameters to provide adequate interaction between the newly formed bone and the implant surface, providing implant stability over time [21,22]. In this study, niobium-containing grafts were tested in vivo in a rat femur model and a higher mineral content was found during the healing process for niobium-containing materials. Considering the microstructure of bone formed, the trabecular structure in BAGNb grafts were adequately formed and comparable to the autogenous bone at 60 days with a slower maturation of bone.

The development of synthetic materials may reduce the need for the harvesting of autogenous bone and improving material's properties may increase the effectiveness of bone formation. In this way, the developed synthetic niobium-containing grafts showed no complications after the animal surgeries. A rat femur model was chosen as a load-bearing model for an initial screening of bone for-



**Fig. 3 – Trabecular parameters of formed bone after 15, 30 and 60 days of surgery.**

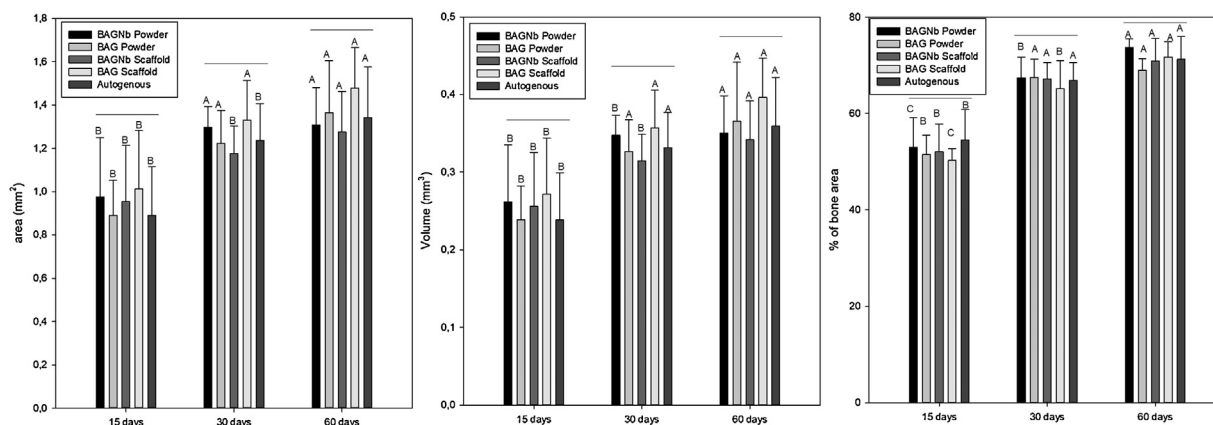


**Fig. 4 – Distribution of mineral density (HU units) along with the defects after 15, 30 and 60 days.**

**Table 1 – Mean and standard deviation of bone density values (HU units) after 15, 30 and 60 days.**

	Bone density (HU units)				
	Powder		Scaffold		Control
	BAGNb	BAG	BAGNb	BAG	Autogenous
15 days	194.64 ( $\pm 11.05$ ) <sup>Bab</sup>	188.27 ( $\pm 10.56$ ) <sup>Cc</sup>	193.36 ( $\pm 10.51$ ) <sup>Bb</sup>	190.40 ( $\pm 9.83$ ) <sup>Cb</sup>	195.73 ( $\pm 7.22$ ) <sup>Aa</sup>
30 days	197.11 ( $\pm 4.17$ ) <sup>Aa</sup>	196.60 ( $\pm 4.88$ ) <sup>Ba</sup>	196.72 ( $\pm 5.88$ ) <sup>Aa</sup>	195.93 ( $\pm 5.94$ ) <sup>Ba</sup>	195.64 ( $\pm 5.71$ ) <sup>Ba</sup>
60 days	197.85 ( $\pm 2.33$ ) <sup>Aa</sup>	201.83 ( $\pm 2.75$ ) <sup>Aa</sup>	196.96 ( $\pm 3.98$ ) <sup>Aa</sup>	201.68 ( $\pm 3.24$ ) <sup>Aa</sup>	199.45 ( $\pm 2.75$ ) <sup>Aa</sup>

Different uppercase letters indicate statistical difference between the same material in different postoperative times; different lowercase letters indicate statistical difference between different materials within the same post-operative time.

**Fig. 5 – The mean and standard deviation of the area, % of area and volume of bone measure after 15, 30 and 60 days after surgery.**

mation [23]. The addition of different concentrations of niobium to bioactive glasses was tested in a previous study with no adverse effects [7,24]. Further, niobium has been used in biomaterial applications for the past few years with no hepatic toxicity and no severe inflammation reported [25,26].

The composition and production approach for synthetic grafts play an important role in bioactivity and degradation [27,28]. In the present study, a rich SiO<sub>2</sub> glass was used and niobium was added in a 1 mol% concentration. Despite the low concentration used, the structure of the glass was modified. The chemical characterization of developed materials showed that niobium was found scattered throughout the matrix without the formation of Si–O–Nb bonding [7]. The main crystalline phase was a hexagonal niobium pentoxide, which is related to the upregulation of cell activity and the increased differentiation of osteoblastic cells [29]. These modifications influenced the ability of these materials to promote bone deposition. In addition, increased BV/TV was observed for BAGNb grafts after 30 days of healing, which may be related to a faster deposition of mineral content in the femur defect. Niobium contributed to the osteogenic activity of materials when a melt-quenching production method was used [24]. This behaviour was observed despite the lower solubility of niobium ions found for melt-derived niobium-containing glasses [30]. The sol–gel route used in this study to synthesize the glasses enables a higher solubility and consequently

higher ion release, especially considering the role of niobium in the glasses' structure, which may contribute to the formation of a high volume of bone [3].

The developed powders and scaffolds present the same chemical and crystalline structures, but differences in total surface area were reported [7]. An increased surface area was observed for scaffolds in the *in vitro* analysis, which was associated with a higher mineralization potential due to the interaction between the material and tissues [7]. The developed scaffolds presented an adequate structure and showed *in vitro* higher mineralization as compared with the powders; however, this behaviour was not found in the present study when scaffolds were compared to powders with the same composition. The BAGNb powders presented higher BV/TV and higher ConnD values after 15 days when compared with the scaffolds of the same composition (Fig. 2A and B;  $p < 0.05$ ). The main advantage of tridimensional scaffolds is the porous structure that promotes easily flow of cells, nutrients, and vascular tissue through the defect [27]. This result shows that the composition, rather than structure, may influence the bone formation. The exact mechanism by which niobium enhances cell activity is still not clarified and further analysis must therefore be conducted in this regard.

The higher mineral content is an important parameter to assess in bone formation, but must not be considered as indicator alone, as the quality of bone is related to the clinical success of bone regenerative treatments [19,31]. Morphome-

tric measurements in tridimensional images were used, as a good correlation with histological analysis was found, leading to an understanding about the maturation of formed bone over the time [32–34]. The higher mineral content observed for BAGNb glasses did not result in enhanced bone quality during the postoperative period. In the early stages of healing (i.e., first 15 days), all materials presented a similar trabecular formation (Tb.N) when compared with that of autogenous bone, but, after 30 and 60 days, autogenous bone presented a higher formation of trabecular structure, which may indicate that maturation was slower for the synthetic materials. More specifically, Tb.Th was higher for BAGNb grafts and for autogenous bone, but only BAGNb powders behaved like autogenous bone after 30 and 60 days of healing. This behavior has been found for other bone substitutes with synthetic [35] and xenogenic [36] grafts. These parameters may influence the mechanical stability. The formation of mature bone is related to the implant stability [21,22] and to increased mechanical properties in bone [37] as no capsule formation may be formed when the implants are in contact with well-formed bone [22]. Although the analysis of new bone formation did not include the evaluation of mechanical properties, the grafting procedures were performed in a load bearing model and no impact on animal mobility or bone fracture was observed.

Synthetic bone substitutes are well-established for use in bone regeneration procedures [14], but few commercial products with this glass composition are available at this time. Improvements in material properties through the modification of composition and production method may enhance the ability of bioactive glasses to promote more effective bone regeneration. The application of niobium-containing bioactive glasses in a rat femur model promoted bone formation comparable to that of the autogenous bone without compromising the quality of the formed bone.

## Funding

This work was supported by FIPE (Fundo de Incentivo à Pesquisa-HCPA). This study was financed in part by the Coordenação de Aperfeiçoamento de Pessoal de Nível Superior - Brasil (CAPES) - Finance Code 001 – scholarship.

## Acknowledgment

The authors are grateful to the team of UEA/HCPA for the support in animal care during the study.

## REFERENCES

- Moreira GS, Machado Alves PH, Esper LA, Sbrana MC, da Silva Dalben G, Neppelenbroek KH, et al. Effect of low-level laser on the healing of bone defects filled with autogenous bone or bioactive glass: in vivo study. *Int J Oral Maxillofac Implants* 2018;33:169–74, <http://dx.doi.org/10.11607/jomi.5900>.
- Pereira RS, Menezes JD, Bonardi JP, Griza GL, Okamoto R, Hochuli-Vieira E. Comparative study of volumetric changes and trabecular microarchitecture in human maxillary sinus bone augmentation with bioactive glass and autogenous bone graft: a prospective and randomized assessment. *Int J Oral Maxillofac Surg* 2018;47:665–71, <http://dx.doi.org/10.1016/j.ijom.2017.11.016>.
- Jones JR. Reprint of: review of bioactive glass: from Hench to hybrids. *Acta Biomater* 2015;23(Supplement):S53–82, <http://dx.doi.org/10.1016/j.actbio.2015.07.019>.
- Hench LL, Paschall HA. Histochemical responses at a biomaterial's interface. *J Biomed Mater Res* 1974;8:49–64, <http://dx.doi.org/10.1002/jbm.820080307>.
- Xynos ID, Hukkanen MV, Batten JJ, Buttery LD, Hench LL, Polak JM. Bioglass 45S5 stimulates osteoblast turnover and enhances bone formation in vitro: implications and applications for bone tissue engineering. *Calcif Tissue Int* 2000;67:321–9.
- Altmann ASP, Collares FM, Balbinot GS, Leitune VCB, Takimi AS, Samuel SMW. Niobium pentoxide phosphate invert glass as a mineralizing agent in an experimental orthodontic adhesive. *Angle Orthod* 2017;87:759–65, <http://dx.doi.org/10.2319/122417-140.1>.
- Balbinot GS, Collares FM, Visioli F, Soares PBF, Takimi AS, Samuel SMW, et al. Niobium addition to sol-gel derived bioactive glass powders and scaffolds: in vitro characterization and effect on pre-osteoblastic cell behavior. *Dent Mater* 2018;34(10):1449–58, <http://dx.doi.org/10.1016/j.dental.2018.06.014>.
- Kushwaha M, Pan X, Holloway JA, Denry IL. Differentiation of human mesenchymal stem cells on niobium-doped fluorapatite glass-ceramics. *Dent Mater* 2012;28:252–60, <http://dx.doi.org/10.1016/j.dental.2011.10.010>.
- Leitune VCB, Collares FM, Takimi A, de Lima GB, Petzhold CL, Bergmann CP, et al. Niobium pentoxide as a novel filler for dental adhesive resin. *J Dent* 2013;41:106–13, <http://dx.doi.org/10.1016/j.jdent.2012.04.022>.
- Carneiro KK, Araujo TP, Carvalho EM, Meier MM, Tanaka A, Carvalho CN, et al. Bioactivity and properties of an adhesive system functionalized with an experimental niobium-based glass. *J Mech Behav Biomed Mater* 2018;78:188–95, <http://dx.doi.org/10.1016/j.jmbbm.2017.11.016>.
- Collares FM, Portella FF, da S Fraga GC, Semeunka SM, de CB Almeida L, da R Santos E, et al. Mineral deposition at dental adhesive resin containing niobium pentoxide. *Appl Adhes Sci* 2014;2:22, <http://dx.doi.org/10.1186/s40563-014-0022-0>.
- Esposito M, Felice P, Worthington HV. Interventions for replacing missing teeth: augmentation procedures of the maxillary sinus. *Cochrane Database Syst Rev* 2014;5:CD008397, <http://dx.doi.org/10.1002/14651858.CD008397.pub2>.
- Nkenke E, Neukam FW. Autogenous bone harvesting and grafting in advanced jaw resorption: morbidity, resorption and implant survival. *Eur J Oral Implantol* 2014;7(Suppl. 2):S203–217.
- Papageorgiou SN, Papageorgiou PN, Deschner J, Götz W. Comparative effectiveness of natural and synthetic bone grafts in oral and maxillofacial surgery prior to insertion of dental implants: systematic review and network meta-analysis of parallel and cluster randomized controlled trials. *J Dent* 2016;48:1–8, <http://dx.doi.org/10.1016/j.jdent.2016.03.010>.
- Starch-Jensen T, Aludden H, Hallman M, Dahlin C, Christensen A-E, Mordenfeld A. A systematic review and meta-analysis of long-term studies (five or more years) assessing maxillary sinus floor augmentation. *Int J Oral Maxillofac Surg* 2017;47(1):103–16, <http://dx.doi.org/10.1016/j.ijom.2017.05.001>.
- Doube M, Kłosowski MM, Arganda-Carreras I, Cordelières FP, Dougherty RP, Jackson JS, et al. BoneJ: free and extensible

- bone image analysis in ImageJ. *Bone* 2010;47:1076–9, <http://dx.doi.org/10.1016/j.bone.2010.08.023>.
- [17] Bi L, Zobell B, Liu X, Rahaman MN, Bonewald LF. Healing of critical-size segmental defects in rat femora using strong porous bioactive glass scaffolds. *Mater Sci Eng C* 2014;42:816–24, <http://dx.doi.org/10.1016/j.msec.2014.06.022>.
- [18] Corsetti A, Bahuschewskyj C, Ponzoni D, Langie R, Santos LAD, Camassola M, et al. Repair of bone defects using adipose-derived stem cells combined with alpha-tricalcium phosphate and gelatin sponge scaffolds in a rat model. *J Appl Oral Sci Rev FOB* 2017;25:10–9, <http://dx.doi.org/10.1590/1678-77572016-0094>.
- [19] Parsa A, Ibrahim N, Hassan B, van der Stelt P, Wismeijer D. Bone quality evaluation at dental implant site using multislice CT, micro-CT, and cone beam CT. *Clin Oral Implants Res* 2015;26:e1–7, <http://dx.doi.org/10.1111/clr.12315>.
- [20] Lundgren S, Cricchio G, Hallman M, Jungner M, Rasmusson L, Sennerby L. Sinus floor elevation procedures to enable implant placement and integration: techniques, biological aspects and clinical outcomes. *Periodontol* 2000;2016(73):103–20, <http://dx.doi.org/10.1111/prd.12165>.
- [21] Zanetti EM, Ciaramella S, Cali M, Pascoletti G, Martorelli M, Asero R, et al. Modal analysis for implant stability assessment: sensitivity of this methodology for different implant designs. *Dent Mater* 2018;34:1235–45, <http://dx.doi.org/10.1016/j.dental.2018.05.016>.
- [22] Akoğlan M, Tatli U, Kurtoğlu C, Salimov F, Kürkçü M. Effects of different loading protocols on the secondary stability and peri-implant bone density of the single implants in the posterior maxilla. *Clin Implant Dent Relat Res* 2017;19:624–31, <http://dx.doi.org/10.1111/cid.12492>.
- [23] Bigham-Sadegh A, Oryan A. Selection of animal models for pre-clinical strategies in evaluating the fracture healing, bone graft substitutes and bone tissue regeneration and engineering. *Connect Tissue Res* 2015;56:175–94, <http://dx.doi.org/10.3109/03008207.2015.1027341>.
- [24] Souza L, Lopes JH, Encarnaçao D, Mazali IO, Martin RA, Camilli JA, et al. Comprehensive in vitro and in vivo studies of novel melt-derived Nb-substituted 45S5 bioglass reveal its enhanced bioactive properties for bone healing. *Sci Rep* 2018;8, <http://dx.doi.org/10.1038/s41598-018-31114-0>.
- [25] Challa VSA, Mali S, Misra RDK. Reduced toxicity and superior cellular response of preosteoblasts to Ti-6Al-7Nb alloy and comparison with Ti-6Al-4V. *J Biomed Mater Res A* 2013;101:2083–9, <http://dx.doi.org/10.1002/jbm.a.34492>.
- [26] Dsouki NA, de Lima MP, Corazzini R, Gáscón TM, Azzalis LA, Junqueira VBC, et al. Cytotoxic, hematologic and histologic effects of niobium pentoxide in Swiss mice. *J Mater Sci Mater Med* 2014;25:1301–5, <http://dx.doi.org/10.1007/s10856-014-5153-0>.
- [27] El-Rashidy AA, Roether JA, Harhaus L, Kneser U, Boccaccini AR. Regenerating bone with bioactive glass scaffolds: a review of in vivo studies in bone defect models. *Acta Biomater* 2017;62:1–28, <http://dx.doi.org/10.1016/j.actbio.2017.08.030>.
- [28] Fernandes HR, Gaddam A, Rebelo A, Brazete D, Stan GE, Ferreira JMF. Bioactive glasses and glass-ceramics for healthcare applications in bone regeneration and tissue engineering. *Materials* 2018;11:2530, <http://dx.doi.org/10.3390/ma11122530>.
- [29] Pradhan D, Wren AW, Misture ST, Mellott NP. Investigating the structure and biocompatibility of niobium and titanium oxides as coatings for orthopedic metallic implants. *Mater Sci Eng C Mater Biol Appl* 2016;58:918–26, <http://dx.doi.org/10.1016/j.msec.2015.09.059>.
- [30] Lopes JH, Magalhães A, Mazali IO, Bertran CA. Effect of niobium oxide on the structure and properties of melt-derived bioactive glasses. *J Am Ceram Soc* 2014;97:3843–52, <http://dx.doi.org/10.1111/jace.13222>.
- [31] Li J, Yin X, Huang L, Mouraret S, Brunski JB, Cordova L, et al. Relationships among bone quality, implant osseointegration, and wnt signaling. *J Dent Res* 2017;96:822–31, <http://dx.doi.org/10.1177/0022034517700131>.
- [32] Bouxsein ML, Boyd SK, Christiansen BA, Guldberg RE, Jepsen KJ, Müller R. Guidelines for assessment of bone microstructure in rodents using micro-computed tomography. *J Bone Miner Res* 2010;25:1468–86, <http://dx.doi.org/10.1002/jbmr.141>.
- [33] Hassumi JS, Mulinari-Santos G, da S Fabris AL, Jacob RGM, Gonçalves A, Rossi AC, et al. Alveolar bone healing in rats: micro-CT, immunohistochemical and molecular analysis. *J Appl Oral Sci* 2018;26, <http://dx.doi.org/10.1590/1678-7757-2017-0326>.
- [34] Müller R, Van Campenhout H, Van Damme B, Van Der Perre G, Dequeker J, Hildebrand T, et al. Morphometric analysis of human bone biopsies: a quantitative structural comparison of histological sections and micro-computed tomography. *Bone* 1998;23:59–66.
- [35] Giuliani A, Manescu A, Larsson E, Tromba G, Luongo G, Piattelli A, et al. In vivo regenerative properties of coralline-derived (Biocoral) scaffold grafts in human maxillary defects: demonstrative and comparative study with beta-tricalcium phosphate and biphasic calcium phosphate by synchrotron radiation X-ray microtomography. *Clin Implant Dent Relat Res* 2014;16:736–50, <http://dx.doi.org/10.1111/cid.12039>.
- [36] Márton K, Tamás SB, Orsolya N, Béla C, Ferenc D, Péter N, et al. Microarchitecture of the augmented bone following sinus elevation with an albumin impregnated demineralized freeze-dried bone allograft (BoneAlbumin) versus anorganic bovine bone mineral: a randomized prospective clinical, histomorphometric, and micro-computed tomography study. *Materials* 2018;11, <http://dx.doi.org/10.3390/ma11020202>.
- [37] Zanetti EM, Pascoletti G, Cali M, Bignardi C, Franceschini G. Clinical assessment of dental implant stability during follow-up: what is actually measured, and perspectives. *Biosensors* 2018;8:68, <http://dx.doi.org/10.3390/bios8030068>.